Production of cuprous oxide, a solar cell material, by thermal oxidation and a study of its physical and electrical properties

A.O. Musa[a], T. Akomolafe[b], M.J. Carter[c],*

[a] *Physics Department, Bayero University, P.M.B. 3011, Kano, Nigeria*
[b] *Physics Department, University of Ilorin, P.M.B. 1515, Ilorin, Nigeria*
[c] *Newcastle Photovoltaics Applications Centre, School of Engineering, University of Northumbria, Newcastle NE1 8St, UK*

Abstract

Cuprous oxide (Cu_2O) is a non stoichiometric defect semiconductor. It is envisaged that this semiconductor could be utilised for the fabrication of low-cost solar cells. Copper foil samples, were oxidised in air between 200°C and 1050°C. The oxide films grown were then investigated by means of both XRD and SEM. The electrical characteristics of Cu_2O films were analysed by means of the hot-probe thermoelectric method, resistivity and mobility measurements. Oxide films formed between 1040°C and 1050°C were observed to consist entirely of Cu_2O and showed p-type semiconductivity while those grown between 200°C and 970°C consists of a mixture of cupric oxide (CuO) and Cu_2O. The CuO layer formed was found to be also p-type semiconducting. Thermodynamic calculations indicate that CuO in the mixed oxide layer could be explained in terms of the oxidation of Cu_2O. Cu_2O layers grown in air without the annealing process gave resistivities in the range 2×10^3–$3 \times 10^3 \, \Omega$ cm. A substantial reduction in the resistivity of the samples was achieved by doping with chlorine during growth and annealing. An average mobility of $75 \, cm^2 \, V^{-1} s^{-1}$, at room temperature, was obtained for eight unannealed Cu_2O samples. This average value increased to $130 \, cm^2 \, V^{-1} s^{-1}$, after doping the samples with chlorine and annealing. © 1998 Elsevier Science B.V. All rights reserved.

Keywords: Cuprous oxide; Thermal oxidation

---

* Corresponding author.

1. Introduction

There is a steady increase in the expenditure of energy resulting from the effect of man's continuous struggle to survive. We consume energy in the form of food, clothing, shelter and tools, and use energy for transportation, heating, cooling and entertainment. A large part of the world's population has not shared the benefit of modern energy utilisation and energy consumption is on the increase for those that have enjoyed the benefits of modern technology. Since the present dependence on fossil fuels will be depleted in the long run, no country can depend on these indefinitely. One aspect which must be considered in connection with the energies of the future is pollution and possible measures to prevent it. This is especially true for nuclear generating plants. These factors, coupled with the increasing world population, create a need for more energy than traditional energy sources can supply. Solar energy utilisation will play a great role in solving the world's energy needs of the future. The direct conversion of sunlight to electricity is likely to be a prime method of the future, assuming that practical economic means of direct conversion can be developed. In operational practice, solar cells have an advantage over thermal conversion modes in that a solar cell responds linearly to the flux. There is no inertia to a solar-cell system, it immediately produces its output at the level appropriate to the solar intensity unlike solar thermal systems that need time to reach operating temperature. Fuel transport and storage problems are eliminated in a photovoltaic-power system. Solar energy can also be efficiently stored in batteries. The future development of photovoltaic cells, such as silicon, is hampered by the present cost of the materials and fabrication. In this work Cu_2O is studied as a potential material for low-cost photovoltaic power generation for the following reasons:

(i) it is nontoxic;
(ii) it has a theoretical solar cell conversion efficiency of 18%;
(iii) there is an abundance of copper;
(iv) the semiconductor layer formation process is simple [1,2].

Even though Cu_2O is one of the oldest semiconducting materials known to solid-state physicists, not much technological improvement has been achieved. As a testimony to this, the highest conversion efficiency using Cu_2O solar cells to date is below 2% [1,3,4] Techniques of doping Cu_2O, to obtain n-type material, do not exist so that homojunction cells of Cu_2O cannot be fabricated. Present research is geared towards Schottky barrier and heterojunction solar cells of Cu_2O. Both frontwall (Cu/Cu_2O) and backwall (Cu_2O/Cu) Schottky barrier solar cells have been studied with promising results. Heterojunction solar cells of ZnO/Cu_2O and CdO/Cu_2O have been reported [4]. Cu_2O is a very good candidate for a top cell in a two (or three) cell stack, because of its large band gap of 2.2 eV. Matched with $CuInSe_2$, for instance, a combination of a 9% Cu_2O cell with a 14% $CuInSe_2$ cell would produce over 20% efficiency as a four-terminal cascade cell.

2. Experimental procedure

2.1. Copper preparation

In the preparation of good-quality Cu_2O the condition of the original copper surface is important. Prior to oxidation, industrial-grade copper sheets (0.1mm thickness and 99.99% purity) were cleaned in 30% nitric acid for 20 s and cut into standard sizes of 4 cm × 2 cm. The samples were then repeatedly rinsed in deionised water and dried with tissue paper.

2.2. Oxidation

The oxidation was carried out at atmospheric pressure in a high-temperature tube furnace. A ceramic crucible was used to hold the samples. When the oxidation temperature was reached, the samples were placed inside the furnace. The temperature and time of oxidation were then varied for both complete and partial oxidation of the samples. Some specimens were oxidised in the presence of HCl vapour. A flow of Ar gas at a pressure of 5×10^{-4} Nm^{-2} from a high-pressure cylinder transports the HCl vapour to the samples during oxidation. After the oxidation, the samples were rapidly quenched in distilled water. The furnace temperature was reduced to 500°C and the samples were given a second heat treatment (annealing) for 90 min, and followed by a second quenching. Black CuO was always formed on the surface of the Cu_2O after the quenching process and for all oxidations carried out below 1040°C. Selective etching to remove CuO was performed using a solution consisting of FeCl, HCl, and 8 M HNO_3 containing NaCl. The last stage of the etching process was carried out in a solution of ammonium persulphate in water.

2.3. Electrical, SEM and XRD measurements

The conductivity type of the oxides were obtained by means of the hot-probe thermoelectric method. The collinear four-point probe method, the van der Pauw and Hall measurements were used to measure the resistivity and mobility of samples. The surface morphology and microstructure of the specimens were analysed using an Hitachi 52400 SEM. The oxide composition was studied using a Siemens D5000 diffractometer.

3. Results and discussion

3.1. Thermal oxidation

Cu_2O has been identified to be stable at limited ranges of temperature and oxygen pressure [5]. It has also been indicated that during oxidation, Cu_2O is formed first and after a sufficiently long oxidation time, CuO is formed [6].

However, at temperatures below 1000°C and at atmospheric pressure, mixed oxides of Cu_2O and CuO are formed as observed from the XRD results. It has been suggested [7] that the probable reactions that could account for the presence of CuO in layers oxidised below 1000°C are

$$2Cu_2O + O_2 \rightarrow 4CuO,$$ (1)

and

$$Cu_2O \rightarrow CuO + Cu.$$ (2)

These two reactions have been evaluated thermodynamically using Gibbs free-energy equation

$$\Delta G = \Delta H - T\Delta S,$$ (3)

where ΔG is the free energy, ΔH is the change in enthalpy, T is the reaction temperature and ΔS is the change in entropy. Using the standard thermodynamic data from the Handbook of Chemistry and Physics [8], ΔG values of -3.70 and $+7.51$ kcal/mol were obtained for reactions given by Eqs. (1) and (2), respectively, at a temperature of 200°C. Thermodynamic considerations therefore show that the presence of CuO in the specimens grown at temperature of 970°C and below could be explained in terms of Eq. (1), i.e., the oxidation of Cu_2O. The oxidation process for Cu at high temperature, at atmospheric pressure, seems to be that the Cu_2O is formed first and it is then gradually oxidised to CuO, depending on the temperature and time of reaction. From Eq. (3), the limiting temperature for the elimination of CuO from the oxide layer was calculated to be 1041°C. This temperature agrees well with the experimental observations recorded in this work.

3.2. SEM analysis

The oxidation process has been identified to involve vacancy diffusion [2] and this results in the formation of voids at the centre plane of the samples. These voids were observed in this work and are visible from the SEM micrograph in Fig. 1. Fig. 2 is the SEM micrograph showing the surface morphology of a copper foil partially oxidised at 970°C for 2 min. The sample was neither annealed nor etched. The surface shows the black CuO coat formed on the violet-red Cu_2O after the oxidation process. The surface morphology is porous and amorphous in nature. The structure formed by this oxidation process is of the form $CuO/Cu_2O/Cu/Cu_2O/CuO$. The hot-probe thermoelectric measurement confirms a p-type CuO. Roos et al. [6] measured a band gap of 1.5 eV for CuO. Herion [9] reported registering a higher open-circuit voltage (V_{oc}) for CuO/Cu_2O heterojunction solar cells compared to frontwall Cu/Cu_2O solar cells and concluded that these cells appear to belong to a basically different class of cells. Roos et al. [6] also suggested the use of CuO/Cu as a solar thermal selective absorber. Figs. 3 and 4 show the SEM micrographs of the morphology and crystallinity of unannealed and annealed CuO surfaces oxidised at 970°C for 2 min after the etching process, respectively. At this temperature there is recrystallisation and normal grain
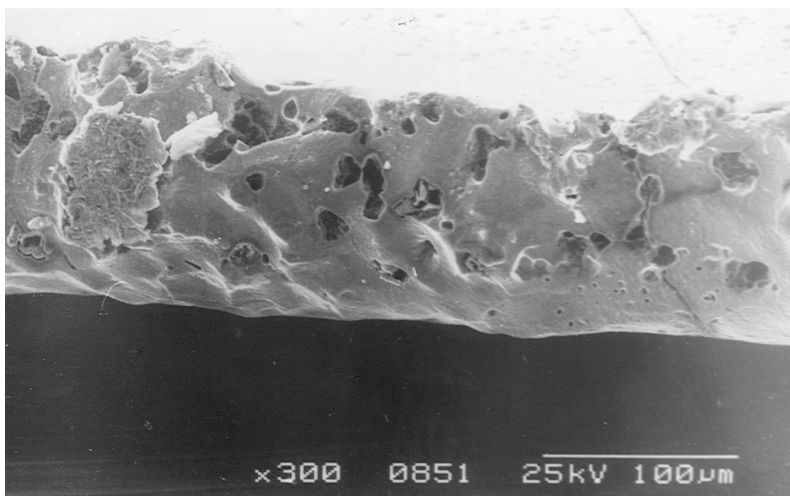
Fig. 1. Cross-sectional micrograph of oxidised sample at 970°C for 10 min and annealed at 500°C for 90 min showing the formation of voids.
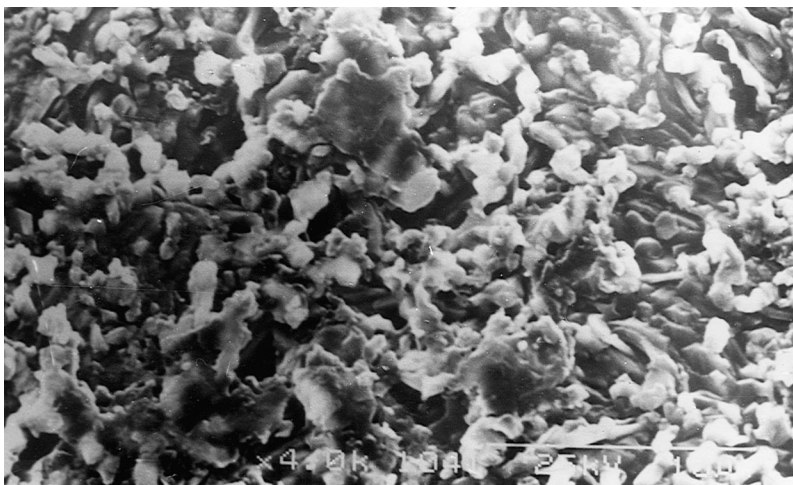

Fig. 2. SEM micrograph of unetched and unannealed sample oxidised at 970°C for 2 min showing CuO coating.

growth in the material resulting in equiaxial grains of Cu_2O. There are gaps observed between the grains, which could be as a result of incomplete grain growth after the oxidation process. The gaps are areas full of dislocations and vacancies. Fig. 4 shows an appreciable compactness and considerable growth of the grains. The disappearance of the gaps between the crystal grains as seen in Fig. 3 is as a result of crystal
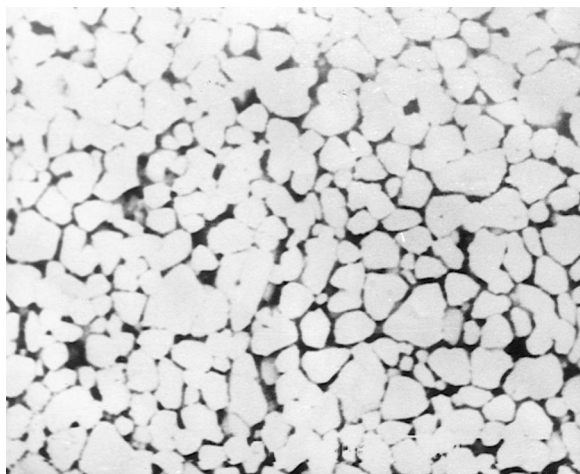
Fig. 3. SEM micrograph of sample oxidised at 970°C for 2 min but unannealed after etching with the first etching solution (FeCl$_3$, HCl and NaCl).

Fig. 4. SEM micrograph of sample oxidised at 970°C for 2 min and annealed after etching with the first etching solution.

growth which occurred during the annealing process. The average grain size for the crystals of the unannealed Cu$_2$O sample in Fig. 3 was estimated to be 0.66 μm while that for the annealed sample in Fig. 4 was estimated to be 0.83 μm. In addition to normal grain growth in this material, there is the annihilation of crystal defects such as vacancies and dislocations. Fig. 5 shows the morphology of a sample oxidised at 970°C for 2 min and etched. Rectangular etch pits and grain boundaries are visible. The pits are rectangular because they occur along the (1 0 0) crystal planes of Cu$_2$O.

Etch-pit formation is an indication of the existence of crystal dislocation during growth [10]. The pits afford a simple method of determining the number of dislocations per square cm. Since etch pits are indications of surface crystal defects, it is a standard practice to polish the surface past these defects for device fabrication. Crystal grains larger than the sample thickness were obtained from this sample.

Fig. 6 shows the cross-sectional view of a sample oxidised at 970°C for 8 min showing the formation of $Cu_2O/Cu/Cu_2O$ structure after the annealing and etching process. The copper layer trapped between the Cu_2O layers on both sides is visible. The very dense crystalline layers on both sides of copper results from annealing the sample at 500°C for 90 min. It is possible to fabricate backwall solar cells of Cu_2O by
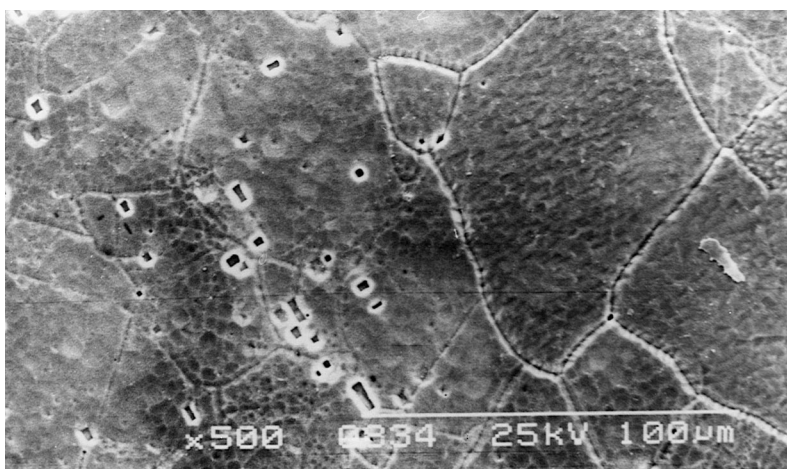

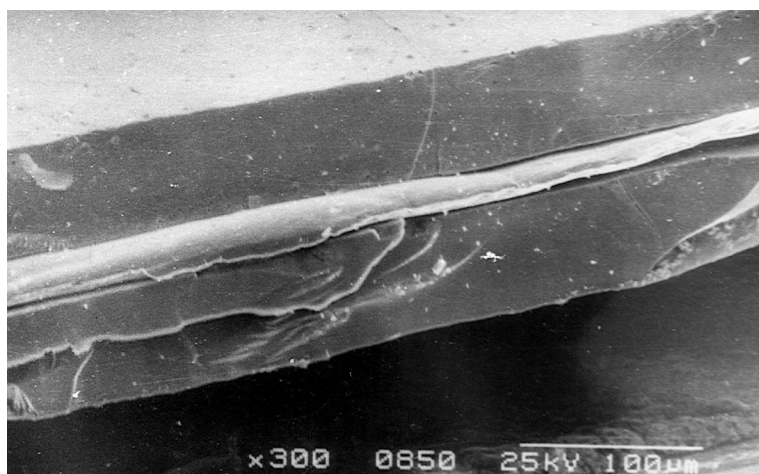Fig. 5. SEM micrograph of an unetched surface of cuprous oxide showing rectangular etch pits.

Fig. 6. Cross-section micrograph of a partially oxidised sample at 970°C for 8 min.

exposing the Cu layer from one side of the $Cu_2O/Cu/Cu_2O$ structure of Fig. 6 to form a Cu_2O/Cu Schottky barrier solar cell.

3.3. XRD analysis

Fig. 7 shows the XRD spectra resulting from the study of oxidised copper samples from 200°C to 1050°C. Essentially, six diffraction lines were generally observed for both complete and partially oxidised copper samples. (Table 1)
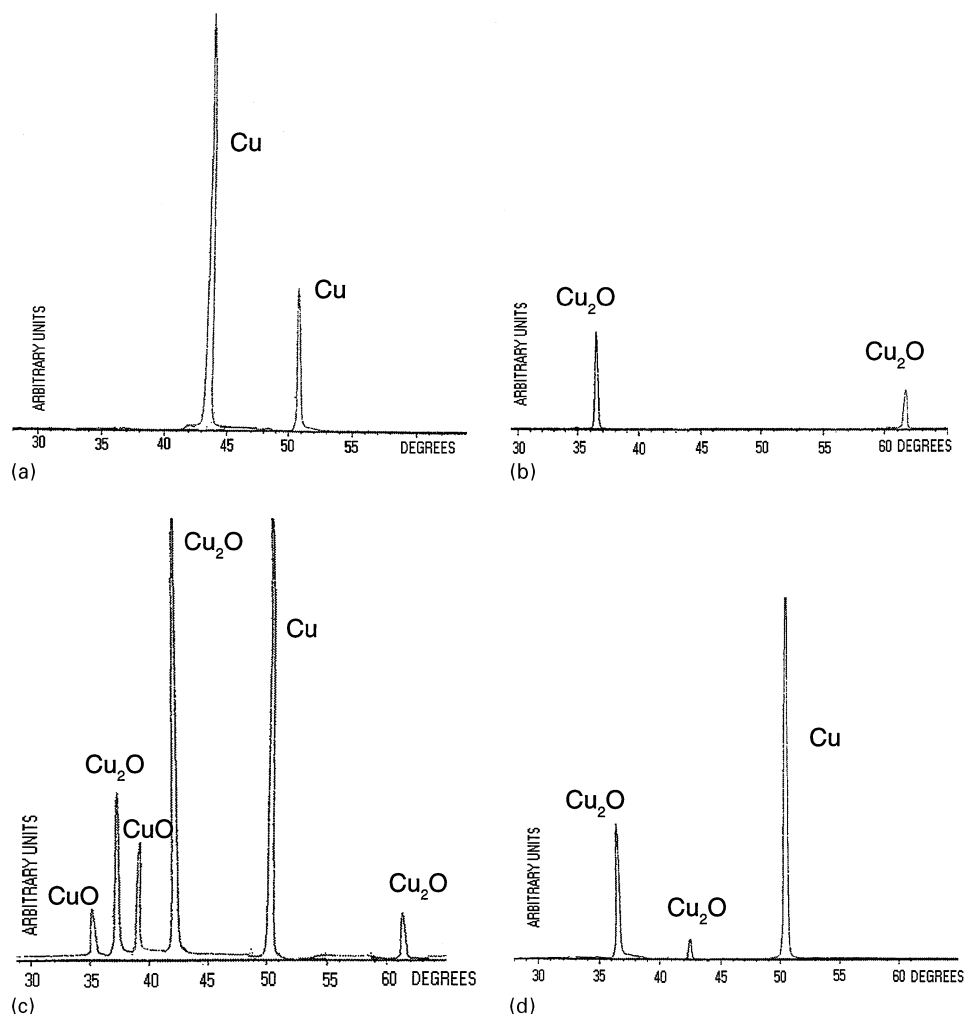

Fig. 7. a. XRD pure copper sample. b. XRD sample oxidised at 1050°C for 2 min. c. XRD sample oxidised at 970°C for 2 min unannealed and unetched. d. XRD sample oxidised at 970°C for 2 min annealed and etched. e. XRD sample oxidised at 970°C for 10 min annealed and etched. f. XRD sample oxidised at 600°C for 20 min unannealed and unetched. g. XRD sample oxidised at 200°C for 72 h unannealed and unetched.
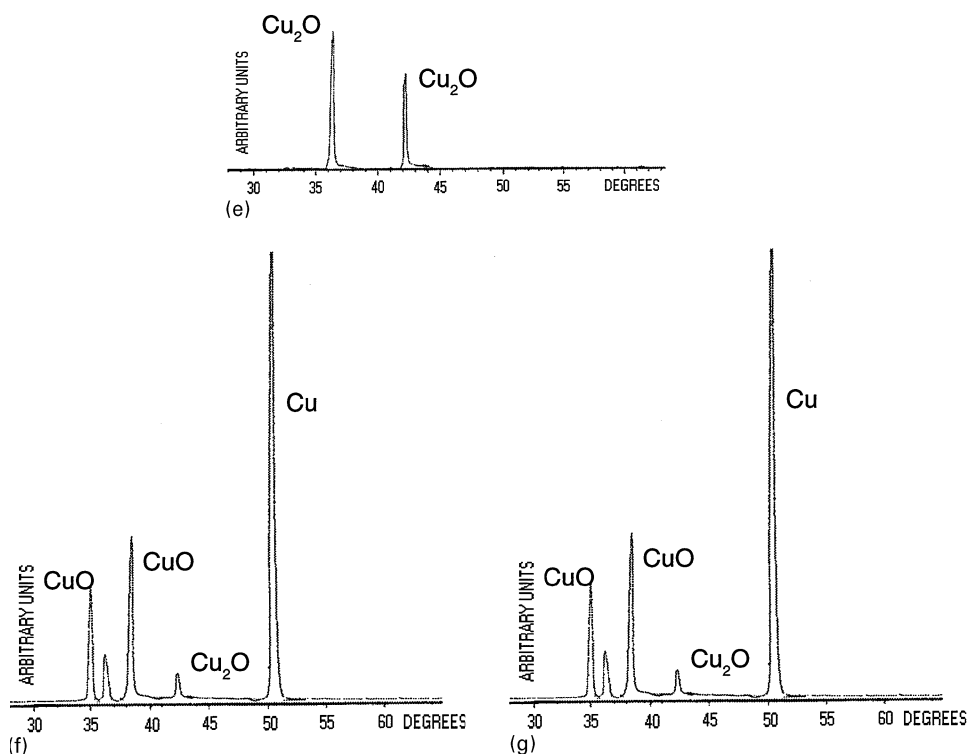
Fig. 7. Continued.

Table 1

2θ deg		
35.5	CuO	($\bar{1}$ 1 1)
36.4	Cu$_2$O	(1 1 1)
38.9	CuO	(2 0 0)
42.3	Cu$_2$O	(2 0 0)
50.5	Cu	(2 0 0)
61.5	Cu$_2$O	(2 2 0)

Fig. 7a shows the spectra for the copper-foil sample before the oxidation process. Fig. 7b is the spectra after the oxidation process at 1050°C for 2 min. The sample was neither etched nor annealed at this stage. This result indicates that samples oxidised at 1050°C consists entirely of Cu$_2$O. Fig. 7c is the spectra of copper oxidised at 970°C at atmospheric pressure for 2 min. The sample was unetched and unannealed. Mixed oxides of CuO and Cu$_2$O are formed in this case. Fig. 7d is the spectra for the same sample shown in Fig. 7c but after annealing at 500°C for 90 min, followed by etching. The XRD results show that the CuO was removed completely by the chemical etching

process. The presence of Cu spectra in both Fig. 7c and Fig. 7d show that only partial oxidation of the copper foil was accomplished within the oxidation time of 2 min. The figures also show the disappearance of the copper spectra at $2\theta = 43.4°$ after the oxidation process. Fig. 7e shows the spectra for an oxidised sample at 970°C for 10 min after the annealing and etching processes. The absence of the Cu peak in this figure is an indication that complete oxidation of the sample was accomplished within the oxidation time. Fig. 7f is for oxidation at 600°C for 20 min. An increased intensity of the diffraction spectra for CuO is observed in this case, which is an indication that more CuO than Cu_2O was formed at this temperature. Fig. 7g shows the spectra for copper foils oxidised for 72 h. No Cu_2O spectra was observed at this temperature as thermodynamically expected.

3.4. Quenching, annealing and etching

The quenching process carried out immediately after the oxidation process was an effective way of rapidly stopping any further oxidation of the samples, once the required oxidation time had been reached. Oxidised samples that were allowed to cool down in air, instead of rapid quenching, were observed to suffer from severe compressive stress. This was made apparent from the observed folding of the samples.

The annealing process was performed to achieve the following:

(i) to heal defects created during the high-temperature oxidation and quenching;

(ii) to lower the resistivity of Cu_2O;

(iii) to convert the polycrystalline Cu_2O obtained after the oxidation process to single or nearly single crystal material.

The etching process was undertaken to selectively remove the black CuO formed in association with Cu_2O for oxidation carried out below 1000°C and for all other Cu_2O specimens, after the annealing process. The micrograph of Fig. 6 showing the very dense crystals of Cu_2O and the XRD result of Fig. 7d show that the objective of carrying out the annealing and etching processes are both achieved.

3.5. Resistivity and mobility measurements

An average resistivity value of $3.7 \times 10^3 \, \Omega \, cm$ was measured for eight unannealed Cu_2O specimens, while an average value of $5.6 \times 10^2 \, \Omega \, cm$ was measured for annealed Cu_2O specimens. Cu_2O obtained by oxidation in the presence of HCl vapour, followed by annealing, gave the least resistivity value of $2.5 \times 10^2 \, \Omega \, cm$. It is suggested that chlorine is the doping agent responsible for lowering the resistivity. Doping of Cu_2O to lower its resistivity has been achieved by means of $MgCl_2$ vapour [2]. It was concluded that the doping agent was chlorine by using an ion microscope mass analyser. This indicated that chlorine was distributed uniformly throughout the Cu_2O grains, while magnesium was present only in the form of precipitates at grain boundaries. The chlorine vapour results from the following reaction:

$$2MgCl_2 + O_2 \rightarrow 2MgO + 2Cl_2 . \tag{4}$$
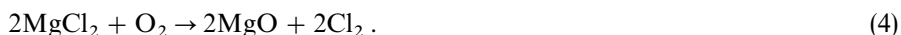
Magnesium results from the decomposition of MgO:

$$2MgO \rightarrow 2Mg + O_2 . \tag{5}$$

It is envisaged in this work that HCl vapour in the presence of the prevailing high temperature would probably decompose, chlorine being heavier might be incorporated in the Cu_2O. If the doping agent is indeed chlorine, then Olsen [2] has suggested that there are two possibilities. First that, chlorine might lead to an acceptor level, if it enters the lattice as a neutral atom at an interstitial site. The second, is that chlorine may replace oxygen substitutionally, thus resulting in a donor level, which in turn could cause copper vacancy production due to charge compensation effects. It is generally accepted that the principal atomic defects responsible for the p-type carriers in Cu_2O are vacancies on the copper sites in the crystal.

The average hole mobility for eight Cu_2O specimens was $130 \, cm^2 \, V^{-1} \, s^{-1}$ at room temperature. This value was measured for specimens that were obtained by oxidation copper in the presence of HCl vapour and with a further anneal of the samples at $500°C$ for 90 min. An average mobility for eight unannealed Cu_2O specimens of $75 \, cm^2 \, V^{-1} \, s^{-1}$ was obtained.

The existence of defects in a semiconductor is expected to impede the flow of charge carriers and hence the mobility. It is therefore expected that hole mobility would be lower for the unannealed samples because of the presence of defects resulting from high-temperature oxidation and quenching. These crystal defects are minimised after the annealing process, resulting in higher values of hole mobility in Cu_2O for the annealed samples.

Mobility of holes in Cu_2O have been measured previously by Vogt in 1930 and Brattain in 1953 [11]. Vogt obtained a value of $100 \, cm^2 \, V^{-1} \, s^{-1}$ at room temperature while Brattain obtained a value of $120 \, cm^2 \, V^{-1} \, s^{-1}$ at the same temperature. The mobility values in this work are in agreement with those found previously.

4. Conclusions

The results of the oxidation process as deduced from both XRD and SEM studies indicate that the oxide layers resulting from oxidation at $1050°C$ consist entirely of Cu_2O. Those grown below $1040°C$ gave mixed oxides of Cu_2O and CuO. It was observed that in general the lower the temperature of oxidation, the lower the amount of Cu_2O was present in the oxide. Thermodynamic considerations indicate that the limiting temperature for the elimination of CuO from the oxide layer was found to be $1040°C$. For thermal oxidation carried out below $1040°C$, Cu_2O is formed first and it is then gradually oxidised to CuO depending on the temperature and time of reaction. Pure unannealed Cu_2O layers grown thermally in air are observed to exhibit higher resistivity and low hole mobility. A significant reduction in resistivity and an increase in mobility values were obtained by oxidising the samples in the presence of HCl vapour, followed by annealing at $500°C$. The SEM studies indicate that the annealing process results in dense polycrystalline Cu_2O layers of increased grain sizes which are appropriate for solar-cell fabrication.

Acknowledgements

References

[1] C. Noguet, M. Tapiero, C. Schwab, J.P. Zielinger, D. Trivich, R.J. Komp, E.Y. Wang, K. Weng, Proc. 1st E. C. Photovoltaic Solar Energy Conf., Luxemburg, 1977, pp. 1170–1181.

[2] L.C. Olsen, F.W. Addis, W. Miller, Solar Cells 7 (1982–1983) 247–279.

[3] J. Herion, B. Natsch, E.A. Nickish, C. Scharl, Proc. 2nd E. C. Photovoltaic Solar Energy Conf., Berlin, 1979, pp. 917–924.

[4] U. Trivich, E.Y. Wang, R.J. Komp, A.S. Kakar, Proc. 13th IEEE Photovoltaic Spec. Conf., Washington, IEEE, New York, 1978, pp. 174–183

[5] A. Roos, B. Karlson, Solar Energy Mater. 7 (1983) 467–480.

[6] A. Roos, T. Chibuye, B. Karlson, Solar Energy Mater. 7 (1983) 453–465.

[7] G.A. Adegboyega, Nigerian J. Renewable Energy 1 (1990) 21–25.

[8] R.I. Weast, Handbook of Chemistry and Physics, 67th ed., Chemical Rubber Company Press, Florida, 1986–1987.

[9] E.A. Herion, E.A. Nickish, G. Scharl, Proc. 14th IEEE Photovoltaic Spec. Conf., San Diego, IEEE, New York, 1982, pp. 453–462.

[10] W.R. Runyan, Semiconductor Measurements and Instrumentation , McGraw-Hill Kogakusha, Tokyo, 1975.

[11] W.H. Brattain, Rev. Mod. Phys. 23 (1951) 203–212.